

# A Numerical Study of a Droplet Impinging on a Liquid Surface

S.Asadi and H.Panahi

**Abstract**—The Navier–Stokes equations for unsteady, incompressible, viscous fluids in the axisymmetric coordinate system are solved using a control volume method. The volume-of-fluid (VOF) technique is used to track the free-surface of the liquid. Model predictions are in good agreement with experimental measurements. It is found that the dynamic processes after impact are sensitive to the initial droplet velocity and the liquid pool depth. The time evolution of the crown height and diameter are obtained by numerical simulation. The critical We number for splashing ( $We_{cr}$ ) is studied for Oh (Ohnesorge) numbers in the range of 0.01–0.1; the results compares well with those of the experiments.

**Keywords**—Droplet impingement; Free surface flows; Liquid crown; Numerical simulation; Thin liquid film.

## I. INTRODUCTION

DROPLET impingement onto a thin liquid film is a phenomenon relevant to many technical applications such as spray cooling, spray painting, corrosion of turbines blades and fuel injection in internal combustion engines; it is also discussed in many natural phenomena such as the erosion of soil and the dispersal of spores and micro-organisms. Considerably less computational studies have been performed on droplet collision onto liquid films. Jossierand and Zelaski [1] proposed a theory predicting the transition between splashing and deposition for impacting droplets on a thin liquid film that was supported by numerical simulation. They employed a potential flow model everywhere except in the small neck region of the developed crown. The effects of viscosity and surface tension on the crown formation were discussed. Their discretization in numerical solution was performed on a Marker and Cell (MAC) grid and the pressure was solved by the explicit projection method. The interface was followed by the VOF method and Piecewise Linear Interface Calculation (PLIC); the capillary force was computed through a variant of the Continuum Surface Stress (CSS) and Continuum Surface Force (CSF) methods. The results presented, however, are more focused on the jet formation at the early stages of the droplet impact on the liquid film. Xie et al [2] studied the process of a single liquid drop impact onto a thin liquid film with a numerical

simulation using moving particle semi-implicit (MPS) method. They validated their model by a comparison with experiments. They found that the dynamic process after impact was sensitive to the thickness of the liquid pool and the initial drop velocity. When the initial drop velocity was low, the drop merged with the liquid film and no strong splash was observed. The numerical results provided, however, show that the particle method does not provide an accurate prediction of the sharp liquid-gas interface especially when the liquid film becomes thin and it breaks up into small droplets.

In this study, the impingement of a droplet onto a thin liquid film is numerically simulated using a modified VOF technique based on the more accurate technique of Youngs' algorithm in an axisymmetric coordinate system. The results of the model are compared with those of the experiments available in the literature. The effects of important processing parameters on the dynamic process of the impingement are studied. Simulations are also performed on very small Oh (Ohnesorge) numbers in the order of 0.001 for which no measurements are reported due to the limitations exist in experiments.

## II. ANALYSIS AND MODELLING

### A. Governing Equations

A schematic of a droplet impingement onto a liquid film is shown in Fig. 1. The mathematical description of the problem is formulated subject to these assumptions:

(i) the droplet is spherical prior to impact, (ii) the liquid is incompressible and Newtonian, (iii) the liquid density, viscosity and surface tension are constant, (iv) the flow during the impact is laminar [3, 4], (v) a single velocity characterizes fluid motion prior to the impact (which precludes considering an internal circulation of the fluid within the droplet prior to the impact), and (vi) the influence of the surrounding gas on the liquid during the impact is negligible (which implies that viscous stresses at the free surface are assumed to be zero).

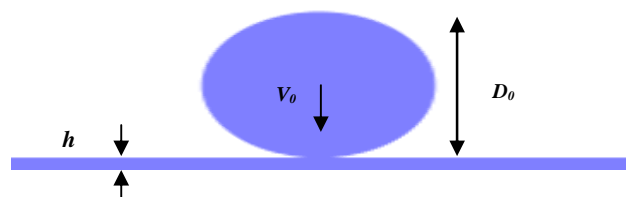


Fig. 1 A schematic of a droplet impingement onto a liquid film.  $D_0$  is drop diameter,  $V_0$  drop velocity before impact and  $h$  liquid film thickness

S.Asadi is associate professor of engineering college of Payame Noor University, Tehran, Iran. (www.pnu.ac.ir , corresponding author to provide phone:0098-21-26120017;e-mail:s\_asadi@pnu.ac.ir , asadiinfo@yahoo.com).

H.Panahi is faculty member of statistics department of Azad University – Lahijan Branch, Lahijan, Iran. (e-mail: panahi@iau-lahijan.ac.ir).

The equations of conservation of mass and momentum in the liquid may then be written as [3, 4]:

$$\nabla \cdot \vec{V} = 0 \quad (1)$$

$$\frac{\partial \vec{V}}{\partial t} + \nabla \cdot (\vec{V}\vec{V}) = -\frac{1}{\rho} \nabla P + \frac{1}{\rho} \nabla \cdot \vec{\tau} + \vec{g} + \frac{1}{\rho} \vec{F}_b \quad (2)$$

The flow equations have been written in an Eulerian frame of reference, and thus a solution of these equations must be coupled with some methodology for following the deforming liquid-gas interface. The VOF technique is applied to track the time evolution of the liquid free surface. A color function,  $f$ , is introduced to represent the volume fraction of liquid in a computational cell. The advection of function  $f$  is governed by [3, 4]:

$$\frac{\partial f}{\partial t} + (\vec{V} \cdot \nabla) f = 0 \quad (3)$$

The volume force,  $\vec{F}_b$ , appearing in Eq. (2), consists of the gravitational force and the surface tension force [5]. To reduce the size of the computational domain, symmetric boundaries are applied when possible. Along a symmetric boundary, fluid velocity obeys slip and no penetration conditions. Boundary conditions are also imposed at the liquid free surface, denoted by subscript  $s$ . The boundary condition on velocity is the zero shear stress condition:

$$\tau_s = 0 \quad (4)$$

and since the surface tension force has been included in Eq. (2), the boundary condition on pressure reduces to:

$$p_s = 0 \quad (5)$$

A boundary condition for  $f$  is unnecessary since  $f$  is a Lagrangian invariant. Initial condition for  $f$  is defined by specifying a droplet diameter  $D_o$ . Fluid velocity within the droplet is characterized by a single impact velocity and the initial pressure within the droplet is defined by the Laplace equation:

$$\vec{V} = \vec{V}_0, \quad P_0 = 4 \frac{\gamma}{D_0} \quad (6)$$

### B. Numerical Procedure

Figure 2 illustrates a typical mesh where velocities are specified at the centre of cell faces and pressure at each cell centre. Equations (1) and (2) are solved with a two-step projection method, in which a forward Euler time discretization of the momentum equation is divided into two steps:

$$\frac{\vec{V}' - \vec{V}^n}{\Delta t} = -\nabla \cdot (\vec{V}\vec{V})^n + \frac{1}{\rho} \nabla \cdot \vec{\tau}^n + \vec{g}^n + \frac{1}{\rho} \vec{F}_b^n \quad (7)$$

$$\frac{\vec{V}^{n+1} - \vec{V}'}{\Delta t} = -\frac{1}{\rho^n} \nabla P^{n+1} \quad (8)$$

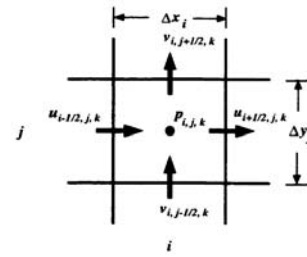


Fig. 2 A 2D control volume, with velocities specified at cell faces, pressure at the cell center

Combining Eq. (8) with Eq. (1) at the new time level  $(n+1)$  yields a Poisson equation for pressure:

$$\nabla \cdot \left( \frac{1}{\rho^n} \nabla P^{n+1} \right) = \frac{1}{\Delta t} \nabla \cdot \vec{V}' \quad (9)$$

The RHS of Eq. (7) is discretized according to the conventions typical of the finite volume method.

The computational domain encompassed the initial droplet and sufficient volume for the liquid film to cover the liquid deformation and subsequent crown formation during the impingement. The mesh size was determined on the basis of a mesh refinement study in which the grid spacing was progressively decreased until further reductions made no significant changes in the predicted crown shape during the impact. The droplet was discretized using a computational mesh, with a uniform grid spacing equal to 1/40 of the droplet radius. Numerical computations were performed on a Pentium 4 computer. Typical CPU times ranged from three to six hours.

### III. RESULTS AND DISCUSSION

The first case considered is that of the collision of a single droplet impinging vertically onto a liquid film with  $D_o=4.2$  mm,  $V_o=5.098$  m/s,  $h=2.1$  mm where  $D_o$  is droplet diameter,  $V_o$  droplet velocity before impact and  $h$  liquid film thickness. Experimental results for this case are available in the literature. Wang and Chen [6] developed a novel technique for studying droplet impact on very thin films of liquid. In their experiment, the glycerol-water solutions were used as the working medium, and the impacting droplet and target liquid were of the same fluid. Viscosity of their solutions was 0.01~0.06 Pa.s which is much higher compared to that of water (i.e. 0.001 Pa. s). These viscous solutions were used to form a very thin liquid film with a uniform thickness. Figure 3 compares images calculated using numerical model with photographs given by Wang and Chen [6] for a case where the density ( $\rho$ ) of the glycerol-water solution was 1200 kg/m<sup>3</sup>, the viscosity ( $\mu$ ) 0.022 Ns/m<sup>2</sup> (Pa.s) and the surface tension ( $\gamma$ ) 0.0652 N/m. Therefore, the Ohnesorge number ( $Oh=\mu/(\gamma\rho D_o)^{0.5}$ ) for this case is 0.0384. As observed from Fig. 3, there is a good qualitative agreement between calculated images and experimental photographs. The formation of corona seen in photographs is well predicted by the numerical model. The time of each image ( $t$ ), measured

from the instant of first contact with the liquid film, is also indicated in the figure. Both simulations and experiments show that after droplet impact, a conical rebound jet is formed that propagates radially outward, forming a thin cylindrical liquid film called corona. The corona reaches its maximum height at  $t=10$  ms after which it starts to subside into the liquid film.

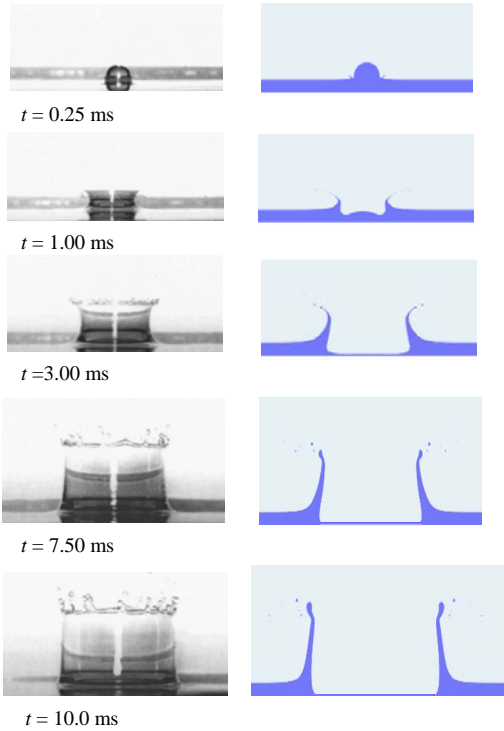


Fig. 3 Computer generated images (3D view and cross-section) and photographs [6] of a 4.2 mm diameter droplet impacting with a velocity of 5.098 m/s onto a liquid film with a thickness of 2.1 mm

The definition of ‘‘crown diameter’’ hides some uncertainties. In fact, as can be observed in Fig. 4, the crown is not usually cylindrical, and the diameter of the external surface varies with the distance from the surface of the film. To account for this uncertainty, two diameters were defined when analyzing the pictures taken from the side: the upper external diameter ( $D_{ue}$  measured at the base of the rim) and the lower external diameter ( $D_{le}$  measured at the crown base), see again Fig. 4.

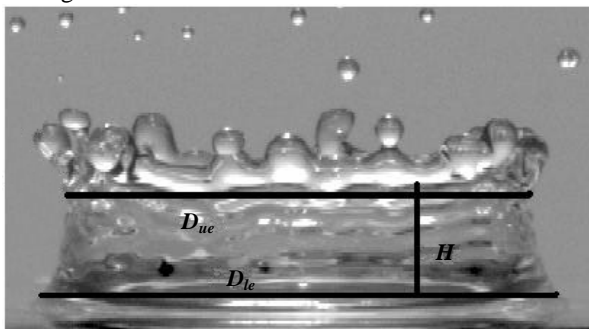


Fig. 4 A 2D control volume, with velocities specified at cell faces, pressure at the cell center

The crown height reaches a maximum value ( $H_{max}^* = H_{max}/D_o$ ) after a certain time ( $t_{max}^* = V_o t_{max}/D_o$ ) from the impact. These two non-dimensional values were calculated from the results of the numerical model for various film thicknesses. Figure 5 shows the variation of the non-dimensional maximum crown height ( $H_{max}^*$ ) against the non-dimensional film thickness ( $h^*$ ) for the impact We numbers ranged from 296 to 1020. It can be seen from this figure that  $H_{max}^*$  is mainly influenced by We and less by  $h^*$ ; therefore,  $H_{max}^*$  can be expressed in terms of We. Using the concept of curve fitting, following equation could be obtained from the figure:

$$H_{max}^* = 0.0025 We \quad (10)$$

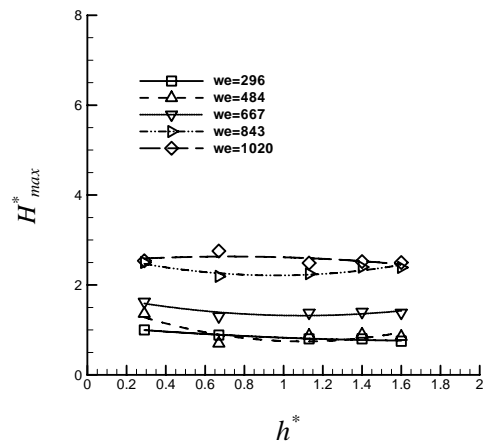


Fig. 5 The variation of the maximum non-dimensional crown height ( $H_{max}^*$ ) against non-dimensional liquid film thickness ( $h^*$ ) for different We numbers ranged from 296 to 1020

The variation of the maximum non-dimensional time ( $t_{max}^*$ ) against the non-dimensional film thickness ( $h^*$ ) is shown in Fig. 6 for the same We numbers as of those for Fig. 5. Similarly, from this figure it is seen that  $t_{max}^*$  is only a function of We where by curve fitting is expressible as:

$$t_{max}^* = 0.0037 We^{1.2} \quad (11)$$

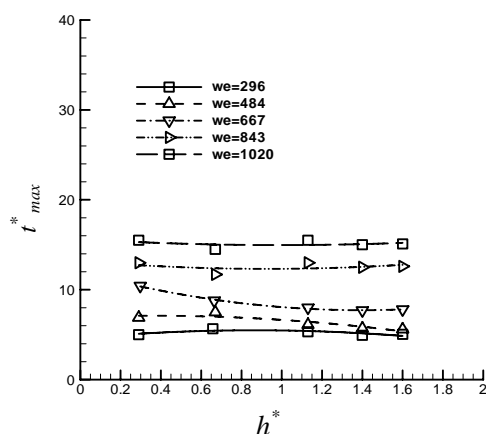


Fig. 6 The variation of  $t_{max}^*$  against non-dimensional film thickness ( $h^*$ ) for different We numbers ranged from 296 to 1020

In the Wang and Chen novel technique [6], viscous fluids  $\{Oh (0.1 \sim 0.1)\}$  were used because of equipment limitations in generating a thin liquid film. As a result, they could not set up their experimental system for a low viscous liquid like water. This is why values for critical impact We numbers in the range of practical Oh numbers (around 0.001) were not reported. Water droplets with a diameter of 2~4.4 mm have Oh equal to 0.00262~0.0018. Predicted critical We number from numerical simulation for such droplets impacting onto a very thin water film are also displayed in Fig. 7 where  $h^* < 0.1$  and Oh ranged from 0.00262 to 0.0018. Figure 7 shows that  $We_{cr}$  is only affected by Oh number; therefore, similar to the last two expressions; a correlation can be obtained by curve fitting as:

$$We_{cr} = 790(1 - e^{-24 Oh}) \quad (12)$$

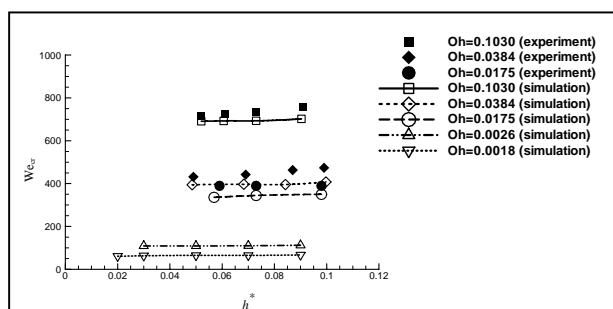


Fig. 7 A comparison between numerical and experimental [6] results for the variations of  $We_{cr}$  against  $h^*$  for three different fluids (60%, 70%, and 80% glycerol-water solution) in the range of  $h^* < 0.1$  and Oh ranged from 0.0175 to 0.1030. The figure also shows the predicted critical We number from numerical simulation for lower Oh numbers equal to 0.00262 and 0.0018 where no measurements are reported in the literature

#### IV. CONCLUSIONS

The collision dynamics of droplet impingement onto a thin liquid film was studied by means of computer simulations.

The Navier–Stokes equations for unsteady, incompressible, viscous fluids in the axisymmetric coordinate system were solved using a control volume method. The volume-of-fluid (VOF) technique was used to track the liquid free-surface. The results of the model were compared and validated with those of the experiments reported in the literature. Non-dimensional maximum crown height and its corresponding time were studied for a range of We numbers. The non-dimensional film thickness had a small effect on the non-dimensional parameters related to the maximum crown height and its corresponding time. Critical We number for splashing ( $We_{cr}$ ) was studied for Oh (Ohnesorge) numbers in the range of 0.01~0.1. A comparison between the numerical results and experimental measurements showed that the model can accurately predict the critical We number. Numerical model was also used to simulate cases with lower Oh number (Oh~0.001) where no measurements are reported due to the limitations in the experiments. The critical We number was found insensitive to the non-dimensional film thickness; it decreased, however, with decreasing Oh number or liquid viscosity.

#### NOMENCLATURE

$D_0$	initial droplet diameter
$f$	liquid volume fraction
$\vec{F}_b$	body force per unit volume
$\vec{F}_{ST}$	surface tension force
$g$	gravitational constant
$\vec{g}$	gravitational acceleration
$H$	crown height
$H^*$	non-dimensional crown height
$H_{max}^*$	maximum non-dimensional crown height
$h$	liquid film thickness
$h^*$	dimensionless film thickness
$k$	total curvature of the interface
$\hat{n}$	unit normal vector
Oh	Ohnesorge number
$P$	pressure
$R^2$	coefficient of determination
$S$	area of free surface
$t$	time
$t^*$	non-dimensional time
$t_{max}^*$	maximum non-dimensional time
$\vec{V}$	velocity vector
$V_0$	droplet velocity before impact
We	Weber number
$We_{cr}$	critical impact Weber number
$\delta$	Dirac delta function
$\vec{x}, \vec{y}$	position vectors
$\Delta t$	time step
$\gamma$	liquid-gas surface tension
$\mu$	dynamic viscosity

$\rho$  density  
 $\tilde{\tau}$  shear stress tensor  
 $\Omega$  volume  
 $\nabla$  del operator

#### Subscripts and Superscripts

i, j, k mesh indices  
n, n+1 time levels  
o initial  
s free surface  
' interim  
\* non-dimensional

#### REFERENCES

- [1] C. Josserand, and S. Zaleski, "Droplet splashing on a thin liquid film," *Phys. Fluids*, 15 (6), p.1650, 2003.
- [2] H. Xie, S. Koshizuka, and Y. Oka, "Modeling of a single drop impact onto liquid film using particle method," *Int. J. Numer. Meth. Fluids*, 45, p.1009, 2004.
- [3] M. Pasandideh-Fard, V. Pershin, S. Chandra, and J. Mostaghimi, "Splat shapes in a thermal spray coating process: simulations and experiments," *J. Thermal Spray Technology*, 11, p.206, 2002.
- [4] M. Bussman, J. Mostaghimi, and S. Chandra, "On a three-dimensional volume tracking model of droplet impact," *Phys. Fluids*, 11 (6), p.1406, 1999.
- [5] J. U. Brackbill, D. B. Kothe, and C. Zemach, "A continuum method for modeling surface tension," *J. Comput. Phys.*, 100, p.335, 1992.
- [6] A. -B. Wang, and C. -C. Chen, "Splashing impact of a single drop onto very thin liquid films," *Phys. Fluids*, 12, p.2155, 2000.